

INTERACTION OF LASER RADIATION WITH MATTER

PACS numbers: 42.62.Cf; 64.70.dj
DOI: 10.1070/QE2009v039n05ABEH013921

Large-scale structures produced on metal surfaces by multiple laser pulses

N.A. Kirichenko

***Abstract*. A mathematical model is constructed to describe the formation of inhomogeneous surface structures 10 – 50 μm in height on metal surfaces exposed to repetitive laser pulses with the following parameters: pulse duration of ~ 20 ns, pulse repetition rate of ~ 10 kHz, pulse intensity in the range $10^7 - 10^8$ W cm^{-2} and beam diameter from 50 to 100 μm. The model takes into account melting of the metal and melt flow over a distorted surface. The surface profile amplitude evaluated in the model agrees with experimental data.**

Keywords: *repetitive laser pulses, interaction of radiation with matter, microstructures, melting, melt flow, mathematical model.*

1. Introduction

In many instances, laser irradiation produces inhomogeneous structures on solid surfaces. Although such structures are sometimes similar in geometry (height, lateral dimensions, profile), the mechanisms underlying their formation depend significantly on incident intensity and pulse duration. The types of surface structures that can be produced by cw, single-pulse and repetitive-pulse exposures have been the subject of several reviews [1 – 4]. It is worth mentioning that, at incident intensities from $\sim 10^5$ to 10^6 W cm^{-2}, quasi-cw laser irradiation may give rise to an interesting effect: deep-penetration (dragger-like) melting [3] due to molten metal ejection from the laser heating zone by the high vapour pressure. Note that, in many instances, theoretical analysis of surface structures was carried out by numerically solving input equations under simplifying assumptions or by examining the onset in the formation of such structures. The latter approach is not always applicable when the parameters of structures in the final stages of their development are sought. Moreover, characteristics of surface structures produced on a target by cw and pulsed (repetitive-pulsed) laser irradiation may differ not only quantitatively but also qualitatively.

The formation of microstructures on a length scale of tens of microns on metal targets exposed to multiple laser pulses was studied by several groups [5 – 8], in particular with the use of a 0.51-μm copper vapour laser.

It was assumed in [9] that, under repetitive-pulsed laser irradiation with an incident intensity from $\sim 10^7$ to 10^8 W cm^{-2} and a pulse duration of $\sim 10^{-8}$ s, the generation of surface structures is mainly due to the melt flow driven by thermocapillary forces. A simple mathematical model was proposed for the initial stages in the formation of inhomogeneous surface structures [10]. The key point of the model is that, in a nonuniform thermal field, thermocapillary forces drive the melt from higher temperature zones to lower temperature zones (where the surface tension is higher). In particular, the melt flow was shown to play a significant role in the stage when the liquid phase persists after the laser pulse.

More detailed studies of the initial stages in the formation of surface structures [11, 12], with all the factors determining the process taken into account, culminated in a mathematical model which involves, as a key step, jointly solving the heat equation (with allowance for melting and vaporisation) and the Navier – Stokes equation for the melt flow. It has been shown that, at incident intensities in the range $\sim 10^7$ to 10^8 W cm^{-2}, the thickness of the forming melt layer is of the order of a micron. The melt persists for a time much longer (by about one order of magnitude) than the laser pulse duration. The maximum melt flow velocity is 200 cm s^{-1}, and the travel distance of the melt during the time it exists is 0.2 μm. Therefore, an individual laser pulse produces relatively small changes in the surface profile. The height of the residual surface profile after a laser pulse (at the conditions under consideration) was shown to be ~ 0.1 μm. In practical applications, however, each point on the target surface is exposed to a large number of pulses ($\sim 10^3$ to 10^4). As a result, the surface profile height may reach tens of microns. Therefore, to assess the effect of multiple pulses, the model must be modified to explicitly take into account changes in the profile of the surface over which the melt flows.

The purpose of this work is to develop a mathematical model for the effect of repetitive laser pulses (in the ranges of parameters indicated above) on the surface profile of a target. A nonlinear evolution equation is obtained which describes surface profile dynamics as a function of the number of laser pulses. It is shown that the formation of inhomogeneous surface structures with profile heights of the same order as those observed in experiments can be understood in terms of a thermocapillary mechanism.

N.A. Kirichenko Wave Research Center, A.M. Prokhorov General Physics Institute, Russian Academy of Sciences, ul. Vavilova 38, 119991 Moscow, Russia; e-mail: nak-49@mail.ru

Received 18 April 2008; revision received 5 August 2008
Kvantovaya Elektronika **39** (5) 442 – 448 (2009)
Translated by O.M. Tsarev

2. Mathematical model

According to [9–12], the main mechanism behind the formation of surface structures at the irradiation parameters indicated above is the irradiation-induced melting of the metal and melt flow over the surface. Thermocapillary forces drive the melt to zones where the temperature is lower and, hence, the surface tension is higher. The melt flow is also influenced by capillary forces, which tend to reduce the surface curvature of the liquid.

To construct a model describing the effect of multiple pulses on the target surface, melting dynamics must first be analysed for a single pulse. This problem was examined in detail in [11, 12]. It was obtained a system of equations describing metal melting and the melt flow in response to a single pulse.

These results show that, under the conditions in question, heat conduction can be considered in a quasi-one-dimensional approximation (only along the normal to the surface). The point is that the heat and melt transport along the surface during an individual pulse is insignificant (and occurs on a length scale of a fraction of a micron or less). The beam radius used in experiments is $x_0 \sim 50$ μm. As mentioned above, the displacement of the melt over the surface in a time period of $\sim 10^{-7}$ s is ~ 0.2 μm. During this time period, heat is transported over a distance $l_T \sim (a\tau)^{1/2} \sim 1$ μm. Therefore, $\Delta x \ll x_0$, $l_T \ll x_0$, which justifies the above approximation.

The problem under consideration includes many parameters, the most essential of which are the irradiation parameters (pulse duration and spatial intensity distribution) and the properties of the target material. For numerical modelling in this study, the shape of an individual pulse is taken in the form

$$I_\tau(t) = I\frac{t}{\tau}\exp\left(-\frac{t}{\tau}\right). \tag{1}$$

For definiteness, the pulse duration τ is taken equal to 20 ns (like in the experiments described in [11, 12]). The radiation wavelength is assumed to be small compared to the characteristic length scale of surface structures, and hence diffraction effects are insignificant. This assumption is justified because the radiation wavelength in the experiments in question was $\lambda \approx 0.5$ μm, whereas the surface structures were tens of microns in size. The target is taken to have the same properties as nickel:

$$\begin{aligned} &m = 9.63 \times 10^{-23}\ \text{g},\ \rho L_\text{m} = 2.66 \times 10^3\ \text{J cm}^{-3},\\ &T_\text{m} = 1728\ \text{K},\ T_\text{b} = 3073\ \text{K},\ \rho = 8.91\ \text{g cm}^{-3},\\ &\rho L_\text{v} = 5.68 \times 10^4\ \text{J cm}^{-3},\ c = 5.49\ \text{J cm}^{-3}\cdot\text{K}^{-1},\\ &k = 0.66\ \text{W cm}^{-1}\cdot\text{K}^{-1},\ \eta = 2.0 \times 10^{-2}\ \text{g cm}^{-1}\ \text{s}^{-1}. \end{aligned} \tag{2}$$

Here m is the atomic mass, L_m is the specific heat of fusion, L_v is the specific heat of vaporisation, T_m and T_b are the melting and boiling temperatures, ρ is density, k is thermal conductivity, c is the thermal capacity, and η is the melt viscosity.

Let the metal surface be initially flat. Consider a two-dimensional (2D) system in which the z coordinate is measured outwards from the undisturbed surface, and the x coordinate is measured along the surface. The incident intensity depends only on x. Such a situation occurs, e.g., when a beam of radius r_0 is incident on the edge of a plate of thickness $\delta \ll r_0$, and the x coordinate is measured along the edge. As shown previously [11, 12], the time variation of the melt layer thickness $z = h(x, t)$ during one of the first laser pulses is described by the equation

$$\frac{\partial h}{\partial t} = u_0(x,t) - \frac{\partial(\bar{v}h)}{\partial x},\quad \bar{v} = \frac{1}{h}\int_0^h v\,\mathrm{d}z. \tag{3}$$

The shape of the surface is then well represented by the local value of h and is determined by both the melting/solidification processes and melt flow. Equation (3) is a continuity equation in the approximation that the melt layer is thin and may slowly move along the surface, $\bar{v} = \bar{v}(x, t)$ is the through-thickness average velocity of the melt flow over the surface, and $u_0(x, t)$ is the rate at which the melt thickness varies through melting/solidification, with the constraint $\int_0^\infty u_0(x,t)\mathrm{d}t = 0$ (which means that the thickness of the melt layer is zero at the beginning and end of the pulse).

The Navier–Stokes equation for a viscous fluid that slowly flows over a flat solid surface has the form [11, 12]

$$\frac{\partial^2 v}{\partial z^2} = \frac{1}{\eta}\frac{\partial p}{\partial x},\quad \eta\left.\frac{\partial v}{\partial z}\right|_{z=h} = \frac{\mathrm{d}\alpha}{\mathrm{d}x},\quad v\big|_{z=0} = 0, \tag{4}$$

where $p = p_0 - \alpha K$ is the pressure in the melt, which takes into account the external pressure (including the vapour pressure) and the capillary (Laplace) pressure $-\alpha K$, due to the surface curvature K, and $\alpha(T)$ is the surface tension. The solid surface is located at $z = 0$. Solving this problem, we obtain

$$v(x,z) = \frac{1}{2\eta}\frac{\partial p}{\partial x}z^2 + \frac{1}{\eta}\left(\frac{\mathrm{d}\alpha}{\mathrm{d}x} - h\frac{\partial p}{\partial x}\right)z. \tag{5}$$

Therefore,

$$\bar{v} = \frac{1}{h}\int_0^h v\,\mathrm{d}z = -\frac{1}{3\eta}h^2\frac{\partial p}{\partial x} + \frac{1}{2\eta}h\frac{\partial \alpha}{\partial x}. \tag{6}$$

Since the local melt thickness in the case of a flat substrate coincides with the coordinate of the corresponding point on the melt surface, $z = h(x)$, the 2D curvature, which is assumed to be small, is given by

$$K \approx \partial^2 h/\partial x^2. \tag{7}$$

The surface tension of the melt, α, depends on the surface temperature. To a good approximation, it can be represented as

$$\alpha(T) \simeq \alpha_0 + \alpha_1(T - T_0),\quad \alpha_1 = \frac{\mathrm{d}\alpha}{\mathrm{d}T} < 0, \tag{8}$$

with the melting point as the initial temperature T_0 (for nickel, $\alpha_0 = 1.6 \times 10^3$ erg cm^{-2} and $\alpha_1 = 0.383$ erg cm$^{-2}\times$ K^{-1}).

Numerical estimates indicate that the duration of the pressure (p_v) pulse produced by the evaporated material is about one order of magnitude shorter than the time period during which the melt exists and flows, and that the pressure pulse causes no significant melt redistribution over the target surface. This is due to the exponential temperature variation

in the pressure: $p_v \sim \exp(-T_v/T)$, where T_v is determined by the heat of vaporisation, and T is the surface temperature, with $T \ll T_v$. Therefore, the vapour pressure of the target material can be left out of consideration.

As pointed out above, the temperature that appears in Eqn (8) can be evaluated with sufficient accuracy based on a 1D problem of radiative heating in which only the heat transport into the metal is taken into account.

All the above allows the sought evolution equation to be simplified, which was done in subsequent calculations.

Using Eqn (1) and a particular value of τ, one can find the surface temperature and melt thickness as functions of time and I [appearing in (1)]: $T(t, I)$ and $h(t, I)$ (without allowance for the melt flow over the surface). This problem was solved previously [11, 12] for the range of irradiation parameters of interest. The results for nickel (τ ns) are presented in Fig. 1.

Substituting (6)–(8) in (3) and solving this equation, one can find the surface profile after melt solidification (according to calculations, at $I \sim 1.5 \times 10^8$ W cm^{-2} the melt persists for $t \sim 20\tau = 400$ ns). Since a single pulse produces only slight changes in the surface profile ($\delta h \sim 0.1$ μm), the effect of the first few pulses can be assessed by summing up those of the individual pulses. The effect of a single pulse can be evaluated under the assumption that the target surface is initially flat.

Turning to the effect of a large number ($\sim 10^2$) of pulses, one must take into account that in this case the surface profile may experience considerable changes. In addition, there are changes, first, in the flow behaviour of the melt (an increase in melt travel distance and changes in capillary and thermocapillary forces) and, second, in absorbed radiation energy (due to local changes in the angle of incidence of the radiation on the surface).

Let the X coordinate be measured along the surface, and the local Z coordinate, orthogonal to X, be measured outwards along the normal to the surface. We also use the x and z coordinates, referred to the original (flat) target surface. If the surface profile (at some instant in time) is $z = h(x)$, then

$$X = \int_0^x \left[1 + (\mathrm{d}h/\mathrm{d}x)^2\right]^{1/2} \mathrm{d}x.$$

Using the curvilinear coordinates X and Y, the Navier–Stokes equation can be written with allowance for the surface curvature (in the approximation of a thin melt layer and slow flow):

$$\frac{1}{1-ZK}\frac{\partial}{\partial Z}\left[(1-ZK)\frac{\partial v}{\partial Z}\right] - \frac{K^2}{(1-ZK)^2}v = \frac{1}{\eta}\frac{\partial p}{\partial X}. \qquad (9)$$

Here, v is the velocity of the melt flow over the surface, and the surface curvature

$$K = \frac{\partial^2 h/\partial x^2}{\left[1 + (\partial h/\partial x)^2\right]^{3/2}} \qquad (10)$$

is not necessarily small.

Let H be the melt layer thickness along the normal to the surface. The Z coordinate in (9) then takes values between zero and H. According to previous calculations [11, 12], $H_{\max} \sim 1$ μm. Therefore, if the radius of curvature is not very small (exceeds several microns), the correction related to curvature K in (9) can be neglected. Under these conditions, it follows from Eqn (9) that

$$\bar{v} = \frac{1}{H}\int_0^H v\,\mathrm{d}Z = -\frac{1}{3\eta}H^2\frac{\partial p}{\partial X} + \frac{1}{2\eta}\frac{\partial \alpha}{\partial X}. \qquad (11)$$

This relation was derived using the boundary conditions

$$\eta\frac{\partial v}{\partial Z}\bigg|_{Z=H} = \frac{\mathrm{d}\alpha}{\mathrm{d}X}, \quad v\big|_{Z=0} = 0.$$

The continuity equation in terms of the X and Z coordinates has the form

$$\frac{\partial H}{\partial t} = u_0 - \frac{\partial(\bar{v}H)}{\partial X}. \qquad (12)$$

Using Eqns (11) and (12), one can find the profile of a thin layer of the melt that flows over a disturbed surface during a single pulse.

Before passing on to a sequence of many pulses, we derive from (11) and (12) an equation for the surface profile at the end of a successive pulse. Since, according to our calculations, the melt exists under the conditions in question for a time of the order of 10^2 ns, at a pulse repetition rate of $\sim 10^4$ Hz (pulse separation of $\sim 10^5$ ns) the melt fully solidifies before the next pulse. Therefore, each pulse

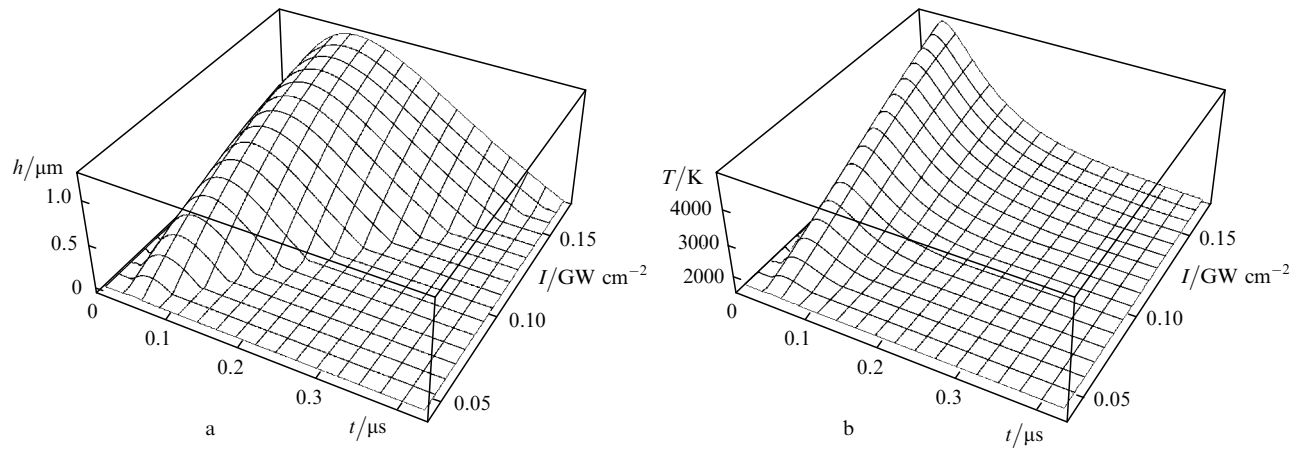

Figure 1. (a) Melt thickness and (b) flat-surface temperature as functions of time and incident intensity for the time dependence (1) with $\tau = 20$ ns.

and the associated melting/solidification cycle can be considered separately from other pulses, and only the surface distortion produced by the previous pulse can be taken into account.

Let us integrate Eqn (12) over the time period during which the melt exists as a result of the nth pulse. Taking into account the relation $\int_0^\infty u_0(x,t)\mathrm{d}t = 0$, we obtain for the change in the melt thickness

$$\Delta H_n = -\frac{\partial}{\partial X}\left(\int_0^\infty \bar{v} H_n \mathrm{d}t\right), \tag{13}$$

where $H_n(x,t)$ is the melt thickness during the nth pulse. Taking into account the change in the slope of the surface with respect to the original plane, $z = 0$, we obtain the change in the surface shape produced by the nth pulse:

$$h_{n+1} - h_n = \Delta H_n \left[1 + (\partial h_n/\partial x)^2\right]^{1/2}. \tag{14}$$

Given that $\mathrm{d}X = \left[1 + (\partial h_n/\partial x)^2\right]^{1/2}\mathrm{d}x$, we have

$$h_{n+1} - h_n = -\frac{\partial}{\partial x}\left(\int_0^\infty \bar{v} H_n \mathrm{d}t\right). \tag{15}$$

Taking into account (11), we obtain the recurrent relation

$$h_{n+1} - h_n = -\frac{\partial}{\partial x}\left\{\frac{1}{3\eta}\frac{B_1(I_n)}{\left[1 + (\partial h_n/\partial x)^2\right]^{1/2}} \times \frac{\partial}{\partial x}\left(\frac{\alpha}{\left[1 + (\partial h_n/\partial x)^2\right]^{3/2}}\frac{\partial^2 h_n}{\partial x^2}\right) + \frac{\alpha_1}{2\eta}\frac{B_2(I_n)}{\left[1 + (\partial h_n/\partial x)^2\right]^{1/2}}\frac{\partial I_n}{\partial x}\right\}, \tag{16}$$

where

$$B_1(I) = \int H^3(t,I)\mathrm{d}t, \quad B_2(I) = \int H^2(t,I)\frac{\partial T(t,I)}{\partial I}\mathrm{d}t \tag{17}$$

are integral moments. These moments can be determined using the time-dependent intensity (1), a particular value of τ and the data presented in Fig. 1. The integration is performed over the time during which the melt exists. This time depends on the local incident intensity, i.e. on the point on the target surface.

The former and latter terms in braces in (16) represent the melt flows due to capillary and thermocapillary forces, respectively. Based on the above, in deriving (16) we neglected the effect of external pressure on the melt flow, taking the pressure in the melt to be equal to the capillary pressure: $p = -\alpha K$. I_n in (14) is the coefficient I in (1) for the pulse under consideration (nth). This coefficient depends on the x coordinate. In particular, for a Gaussian laser beam we have

$$I = I(x) = I_\mathrm{m}\exp\left(-x^2/x_0^2\right). \tag{18}$$

This approach makes it possible to examine the effect of radiation whose intensity may vary from pulse to pulse, provided the time-dependent intensity of each pulse follows Eqn (1) with sufficient accuracy and with the same value of τ.

Finally, taking into account that the surface profile varies little from pulse to pulse and taking in this approximation the pulse number n to be a continuous variable, we obtain from (16) the sought evolution equation for the surface profile:

$$\frac{\partial h}{\partial n} = -\frac{\partial}{\partial x}\left\{\frac{1}{3\eta}\frac{B_1(I)}{\left[1 + (\partial h/\partial x)^2\right]^{1/2}} \times \frac{\partial}{\partial x}\left(\frac{\alpha}{\left[1 + (\partial h/\partial x)^2\right]^{3/2}}\frac{\partial^2 h}{\partial x^2}\right) + \frac{\alpha_1}{2\eta}\frac{B_2(I)}{\left[1 + (\partial h/\partial x)^2\right]^{1/2}}\frac{\partial I}{\partial x}\right\}. \tag{19}$$

Consider now the functions $B_1(I)$ and $B_2(I)$. Note first of all that an important role is played by the absorbed radiation energy, which depends on the angle θ between the incident beam and the normal to the surface. In the simplest case, when the angular dependence of the absorption power is neglected (in the case of unpolarised radiation, this is justified in a relatively wide angular range), there remains a 'geometric' factor related to the increase in spot size on the surface with increasing angle of incidence. Therefore, B_1 and B_2 are, in fact, functions of

$$I_\mathrm{abs} = I\cos\theta = \frac{I}{\left[1 + (\partial h/\partial x)^2\right]^{1/2}}, \tag{20}$$

where I is the coefficient in (1), determining the radiation intensity absorbed at normal incidence. Hereafter, we assume that the normal incidence absorption power $A(0)$ is included in I. If the angular dependence of the absorption power is taken into account in explicit form, the following approximation for the absorption power works well in the case of unpolarised radiation at not too large angles of incidence [4]:

$$A(\theta) = \frac{A(0)}{2}\left(\cos\theta + \frac{1}{\cos\theta}\right).$$

Therefore,

$$I_\mathrm{abs} = I\frac{A(\theta)}{A(0)}\cos\theta = \frac{1}{2}I\left[1 + \frac{1}{1 + (\partial h/\partial x)^2}\right]. \tag{21}$$

At not too large angles of incidence, Eqns (20) and (21) give similar results.

Further, since melting occurs only when the surface temperature during the pulse exceeds the melting temperature T_m, there is a threshold intensity below which no melting occurs, that is,

$$H = 0 \ \text{ for } \ I_\mathrm{abs} \leqslant I_\mathrm{th}.$$

Estimates indicate that, for $I_\mathrm{abs} \to I_\mathrm{th}$ (and of course for $I_\mathrm{abs} > I_\mathrm{th}$),

$$B_1(I) \sim (I_\mathrm{abs} - I_\mathrm{th})^4, \quad B_2(I) \sim (I_\mathrm{abs} - I_\mathrm{th})^3, \tag{22}$$

where I_abs is related to I by (20) [or (21)].

I_th can be estimated from the fact that, at this absorbed energy (at normal incidence), the maximum surface temperature reaches T_m. Calculations indicate that, at a pulse duration of 20 ns, $I_\mathrm{th} = 4.92 \times 10^7$ W cm^{-2} for a material having the same properties as nickel. By normalising the intensity to I_th and expressing all linear dimensions in microns, Eqn (19) can be brought to the form

$$\frac{\partial h}{\partial n} = -\frac{\partial}{\partial x}\left\{ \frac{b_1(q)}{\left[1+(\partial h/\partial x)^2\right]^{1/2}} \times \frac{\partial}{\partial x}\left(\frac{1}{\left[1+(\partial h/\partial x)^2\right]^{3/2}} \frac{\partial^2 h}{\partial x^2} \right) - \frac{b_2(q)}{\left[1+(\partial h/\partial x)^2\right]^{1/2}} \frac{\partial q}{\partial x} \right\}. \tag{23}$$

For b_1 and b_2, we obtain the following approximate expressions:

$$\begin{aligned} b_1(q) &= 11.06967(q-1)^4 - 4.14200(q-1)^5 \\ &\quad - 0.06344(q-1)^6 + 0.12525(q-1)^7, \\ b_2(q) &= 8.03590(q-1)^3 - 2.08703(q-1)^4 \\ &\quad - 1.46955(q-1)^5 + 0.45846(q-1)^6 \text{ for } q > 1, \\ b_1(q) &= 0,\ b_2(q) = 0 \text{ for } q \leqslant 1. \end{aligned} \tag{24}$$

Here,

$$q(x) = \frac{I_{\text{abs}}(x)}{I_{\text{th}}} = \frac{I(x)/I_{\text{th}}}{\left[1+(\partial h/\partial x)^2\right]^{1/2}}. \tag{25}$$

The functions $b_1(q)$ and $b_2(q)$ are well represented by expressions (24) in the intensity range $1 \leqslant q \leqslant 3.45$, or $I_{\text{th}} \leqslant I_{\text{abs}} \leqslant I_{\max}$, where $I_{\max} = 1.7 \times 10^8$ W cm^{-2}. The $b_1(q)$ and $b_2(q)$ curves are presented in Fig. 2.

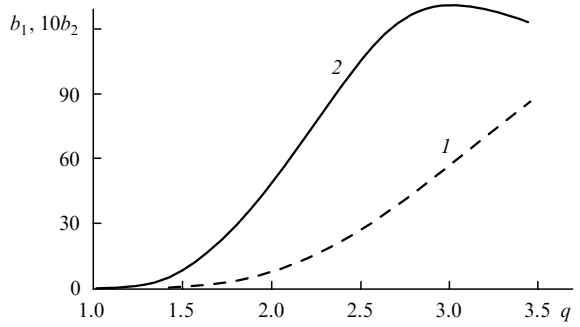

Figure 2. (*1*) $b_1(q)$ and (*2*) $b_2(q)$ curves.

3. Numerical modelling results

Equation (23), supplemented by expressions (24) and (25), is an inhomogeneous nonlinear partial differential equation of order no greater than four. However, by virtue of the constraint

$$B_1(I) = B_2(I) = 0 \text{ for } I_{\text{abs}} < I_{\text{th}}, \text{or}$$

$$b_1(q) = b_2(q) = 0 \text{ for } q < 1,$$

it degenerates into the trivial equation $\partial h/\partial t = 0$ in regions where no melting occurs. This degeneracy may also take place where the incident intensity is initially high enough to cause melting. The point is that the surface distortion increases during melting, which may eventually lead to $q \leqslant 1$, or

$$\frac{I}{\left[1+(\partial h/\partial x)^2\right]^{1/2}} \leqslant I_{\text{th}}.$$

As a consequence, there appear 'frozen' regions in the intensely heating zone. The reduction in the order of Eqn (23) in some points and regions considerably complicates numerical analysis of this equation. The difficulties involved can be partially alleviated by using appropriate numerical implementation and improving the calculation accuracy.

Figure 3 illustrates the surface shape after $n = 10$, 50 and 100 pulses with the Gaussian intensity profile given by (18) and with parameters

$$x_0 = 45 \text{ μm and } I_{\text{m}} = 1.7 \times 10^8 \text{ W cm}^{-2}. \tag{26}$$

The surface was initially flat. Figure 4 shows the time dependences of the maximum and minimum deviations from the initial (zero) level.

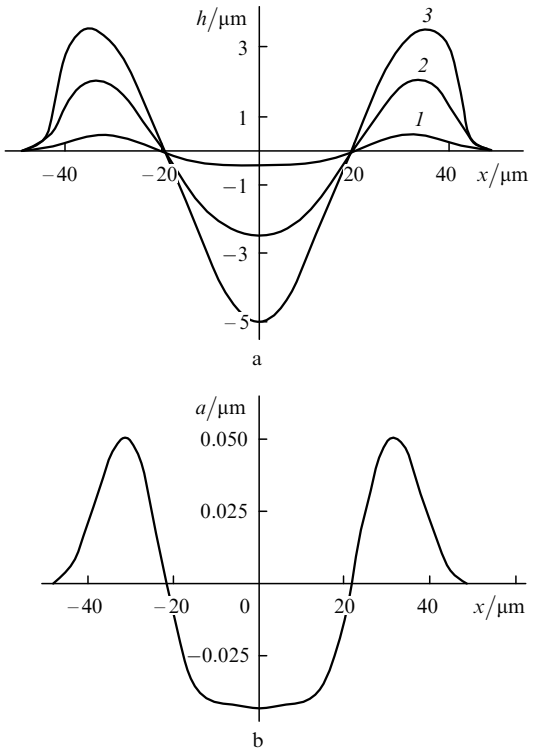

Figure 3. (a) Surface profiles produced by $n = 10$ (*1*), (*2*) 50 and (*3*) 100 pulses with a Gaussian intensity profile; (b) surface distortion (per pulse) by the first few pulses.

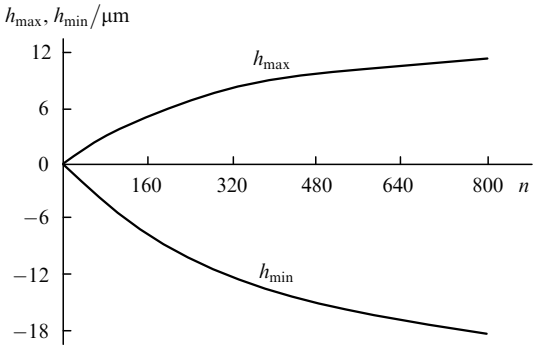

Figure 4. Dynamics of maxima ($h_{\max}$) and minima ($h_{\min}$) in the surface profile in relation to the number of laser pulses; same parameters as in Fig. 3.

The resultant surface profile is very stable. In particular, even if the original surface is distorted, irradiation will produce a surface profile similar to those in Fig. 3. As an example, Fig. 5 illustrates the dynamics of the surface profile (under the same irradiation conditions as in Figs 3 and 4) for an initial surface distortion of the form

$$h_0(x) \equiv h(x,0) = 5\cos\left(\frac{5x}{2x_0}\right),$$

where h_0 is in microns.

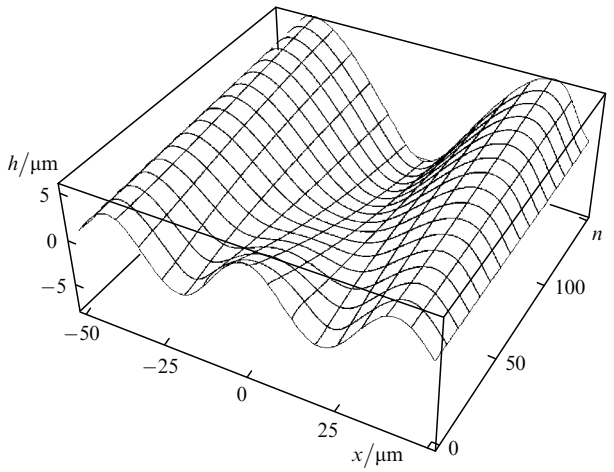

Figure 5. Dynamics of an initially distorted surface profile exposed to multiple laser pulses.

It should be emphasised that the calculated profile height agrees with the relevant experimental data [5–9].

4. Approximate solutions

It follows from the structure of Eqns (23)–(25) that the process comprises three characteristic stages.

In the first stage, the slope of the surface is insignificant: $|\partial h/\partial x| \ll 1$. The surface curvature (10) is also small. Therefore, we can take $[1+(\partial h/\partial x)^2]^{1/2} \approx 1$ and neglect capillary forces [the first term in braces in (23)]. Equation (23) then simplifies to

$$\frac{\partial h}{\partial n} = \frac{\partial}{\partial x}\left[b_2(q)\frac{\partial q}{\partial x}\right] \equiv a(x),$$

or

$$\frac{\partial h}{\partial n} = -\frac{\alpha_1}{2\eta}\frac{\partial}{\partial x}\left[B_2(I)\frac{\partial I}{\partial x}\right] \equiv a(x). \tag{27}$$

This equation has a trivial solution:

$$h(x,n) = a(x)n. \tag{28}$$

The initial linear rise in surface profile amplitude with increasing number of pulses is well seen in Fig. 4. Relation (28) can be used to find the surface profile for an arbitrary beam profile. As an example, Fig. 6 shows a flat-top beam profile of the form

$$q(x) = q_0\frac{1+\exp(-x_0^2/w^2)}{1+\exp\left[(x^2-x_0^2)/w^2\right]} \tag{29}$$

(with parameters $w = 0.5x_0$, $x_0 = 45$ μm and $q_0 = 3.45$) and the corresponding $a(x)$ profile. It can be seen that, in this stage, the surface profile may reflect rather fine details of the intensity distribution (represented by the second derivative with respect to the coordinate). Calculations show however that, in the case of profile (29), during further exposure the surface shape approaches that in Fig. 3a (which requires ~ 300 pulses).

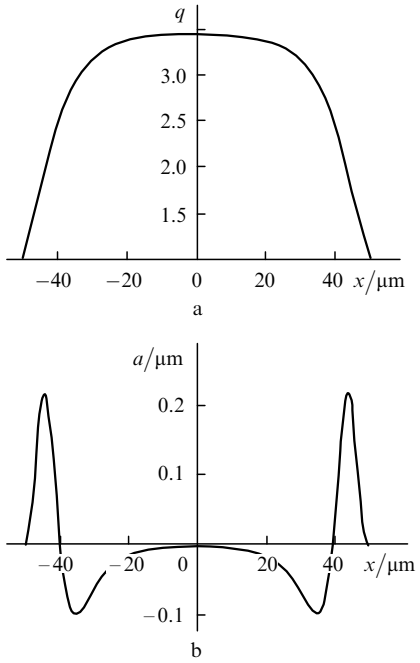

Figure 6. (a) Flat-top beam profile given by (29) and (b) the corresponding distortion a of the surface profile (per pulse).

Expressions (27) and (28) can easily be generalised for a 2D intensity profile. To this end, it is sufficient to rewrite Eqn (27) in the form

$$\frac{\partial h}{\partial n} = -\frac{\alpha_1}{2\eta}\nabla_2\left[B_2(I)\nabla_2 I\right] \equiv a(x,y). \tag{30}$$

Here, ∇_2 is the 2D gradient operator in terms of the x and y coordinates on the target surface. Accordingly, we obtain $h(x,y,n) = a(x,y)n$.

In the second stage, capillary forces come into play, but the slope of the surface remains low: $|\partial h/\partial x| \ll 1$. Accordingly, Eqn (23) contains no nonlinear terms and is inhomogeneous:

$$\frac{\partial h}{\partial n} = -\frac{\partial}{\partial x}\left[\frac{\alpha}{3\eta}B_1(I)\frac{\partial^3 h}{\partial x^3} + \frac{\alpha_1}{2\eta}B_2(I)\frac{\partial I}{\partial x}\right]. \tag{31}$$

In this stage, the development of surface inhomogeneities is inhibited by capillary forces, which tend to reduce the surface curvature. Moreover, instead of a flat-bottom crater (Fig. 3b), a deep hole is produced (Fig. 3a), similar to that in the keyhole melting regime but due to a fundamentally different mechanism.

In the third stage, the surface profile amplitude is so large that a significant role is played by the reduction in absorbed radiation due to the increase in the angle of incidence. Equation (23) is then essentially nonlinear and

involves singular regions of variables. This stage is very difficult to study analytically or numerically. Quantitatively, it begins at $|\partial h/\partial x| \sim 1$. The necessary number of pulses estimated using relation (28) is $n \sim (a'_{\max})^{-1}$. For the Gaussian beam profile given by (18), $a'_{\max} \sim 2 \times 10^{-3}$ (which can be estimated from Fig. 3). Therefore, the third stage begins at $n \sim 500$. This estimate is supported by numerical simulation. It should be emphasised however that, strictly speaking, the nonlinear stage begins at different instants in different points on the target surface. The transition first occurs at the periphery of the beam, where the heating conditions are closer to the threshold. Next, the threshold is reached at a distance $\sim x_0/2$ from the centre of the beam, etc.

An interesting consequence of the above is the inverse problem: the possibility of producing a predetermined $h(x)$ profile. To this end it is sufficient to produce an intensity profile, $I(x)$, that will ensure the necessary function $a(x)$. Using Eqns (27) and (28), one can then determine the number of pulses needed to obtain therequired $h(x)$ profiles.

5. Conclusions

The mathematical model constructed in this work accounts for the characteristic shape and length scale (amplitude and slope) of inhomogeneous surface structures produced on metallic targets by multiple laser pulses at incident intensities from $\sim 10^7$ to 10^8 W cm^{-2} and beam diameters from ~ 50 to 100 μm. Analysis of the model indicates that thermocapillary forces play a central role in the formation of surface structures during the first few hundred pulses. At the same time, in the final stages of the process the surface profile is determined not only by capillary forces but also by the changes in absorbed energy due to the increase in the slope of the surface. The length scale of the surface structures evaluated in the model agrees with experimental data. An evolution equation is derived which directly (without intermediate calculations of the temperature field and melt flow velocity) determines the surface profile produced by a sequence of laser pulses.

The model can be generalised to include a variety of factors, such as an arbitrary 2D intensity distribution and beam scanning over the target surface.

Acknowledgements. I am grateful to G.A. Shafeev, A.V. Simakin and S.M. Pershin for many useful discussions.

References

1. Anisimov S.I., Khokhlov V.A. *Instabilities in Laser-Matter Interaction* (Boca Raton, London, Tokyo: CRC Press, Inc., 1995).
2. Bunkin F.V., Tribel'skii M.I. *Usp. Fiz. Nauk*, **130**, 2 (1980).
3. Bäuerle D. *Laser Processing and Chemistry* (Berlin, Heidelberg, New York: Springer-Verlag, 2000).
4. Karlov N.V., Kirichenko N.A., Luk'yanchuk B.S. *Lazernaya Termokhimiya* (Laser Thermochemistry) (Moscow: TsentrKom, 1995).
5. Sánchez F., Morenza J.L., Aguiar R., Delgado J.C., Varela M. *Appl. Phys. Lett.*, **69**, 620 (1996).
6. Her T.H., Finlay R.F., Wu C., Deliwala S., Mazur E. *Appl. Phys. Lett.*, **73**, 1673 (1998).
7. Pedraza A.J., Fowlkes J.D., Lowndes D.H. *Appl. Phys. Lett.*, **74**, 2322 (1999).
8. Voronov V.V., Dolgaev S.I., Lavrishchev S.V., Lyalin A.A., Simakin A.V., Shafeev G.A. *Kvantovaya Elektron.*, **30** (8), 710 (2000) [*Quantum Electron.*, **30** (8), 710 (2000)].
9. Dolgaev D.I., Lavrischev S.V., Lyalin A.A., Simakin A.V., Voronov V.V., Shafeev G.A. *Appl. Phys. A*, **73**, 177 (2001).
10. Dolgaev S.I., Kirichenko N.A., Simakin A.V., Shafeev G.A. *Kvantovaya Elektron.*, **34**, 771 (2004) [*Quantum Electron.* **34**, 771 (2004)].
11. Dolgaev S.I., Kirichenko N.A., Simakin A.V., Shafeev G.A. *Kvantovaya Elektron.*, **37**, 645 (2007) [*Quantum Electron.*, **37**, 645 (2007)].
12. Dolgaev S.I., Kirichenko N.A., Simakin A.V., Shafeev G.A. *Appl. Surf. Sci.*, **253**, 7987 (2007).